Geoderma 432 (2023) 116424

Contents lists available at ScienceDirect

Geoderma

journal homepage: www.elsevier.com/locate/geoderma

Dry rainfed conditions are key drivers of the effect of conservation tillage and a nitrification inhibitor on N fate and N_2O emissions: A field ^{15}N tracing study

Sandra García-Gutiérrez [a,b,*], Guillermo Guardia [a,b], Mónica Montoya [a,b,c], Antonio Vallejo [a,b], Laura M. Cardenas [d], Sonia García-Marco [a,b]

[a] Departamento de Química y Tecnología de Alimentos, Escuela Técnica Superior de Ingeniería Agronómica, Alimentaria y de Biosistemas, Universidad Politécnica de Madrid, Ciudad Universitaria, Madrid 28040, Spain
[b] Centro de Estudios e Investigación para la Gestión de Riesgos Agrarios y Medioambientales (CEIGRAM), Universidad Politécnica de Madrid, Madrid 28040, Spain
[c] Departamento de Biología, Facultad de Ciencias, Universidad Autónoma de Madrid, Campus de Cantoblanco, Madrid, Spain
[d] Net Zero and Resilient Farming, Rothamsted Research, North Wyke, Okehampton, Devon EX20 2SB, United Kingdom

ARTICLE INFO

Handling Editor: Daniel Said-Pullicino.

Keywords:
Enhanced-efficiency fertilizers
Crop residue management
Mediterranean agroecosystems
Gross nitrogen transformation rates
$^{15}N_2O$
Nitrogen use efficiency

ABSTRACT

The sustainability of rainfed crops under semiarid conditions is threatened by low plant nitrogen (N) recovery as well as the potential loss of reactive N to the environment. A field ^{15}N tracing experiment on barley (*Hordeum vulgare* L.) under rainfed conditions was carried out to study how different tillage management practices and the use of the nitrification inhibitor DMPSA affected the fate of N. The experiment consisted of a factorial combination of tillage (i.e., no tillage, NT, and conventional tillage, T) and fertilizer treatments (unfertilized control and ammonium nitrate, AN, with or without DMPSA). Single-labelled ammonium nitrate ($^{15}NH_4NO_3$, ^{15}AN, or $NH_4^{15}NO_3$, $A^{15}N$) was applied at top-dressing to microplots at a rate of 80 kg N ha^{-1}. Our results show out that DMPSA modulates the nitrification process from both fertilizer-N and endogenous soil-N (which was the main contributor to plant N uptake and N_2O emissions), affecting soil residual N at the end of the cropping period (i.e., higher topsoil retention of ^{15}AN in DMPSA-amended plots). Generally, cumulative N_2O emissions from fertilizer were derived from ^{15}AN rather than from $A^{15}N$, thus confirming the site-specific choice of the source of synthetic N as an effective N_2O mitigation strategy. Two months after harvest, a rewetting event produced a remarkable N_2O emission peak that drove total cumulative N_2O emissions and was also mainly derived from endogenous N. These results suggest that dry seasons could decrease N_2O losses after fertilization while causing critical peaks after rewetting, thus potentially limiting the effectiveness of mitigation strategies. The average plant N recovery from the synthetic fertilizer was 22.6%, while the use of DMPSA combined with NT enhanced plant N uptake from endogenous soil-N. This could be a result of the improved crop development and plant N acquisition under NT, consistent with the decrease of soil N retention for $A^{15}N$ in the deeper layer at the end of the experiment in the nontilled plots. This study contributes to the mechanistic understanding of the effect of nitrification inhibitors and tillage on N_2O emissions, soil N dynamics and N plant recovery, revealing relevant effects of both management strategies and a critical role of endogenous soil-N under dry rainfed conditions. It can be concluded that, under the conditions of our study, combining DMPSA with NT could help to improve plant N recovery, thus resulting in positive impacts on reactive N loss and climate change mitigation and adaptation.

1. Introduction

Nitrogen (N) is, together with water, one of the most important crop yield-limiting factors (Quemada et al., 2020). The expected increases in human population and consumption during future decades will increase the use of synthetic N fertilizers. Fertilized soils are identified as the largest anthropogenic contributor to nitrous oxide (N_2O) emissions (Smith et al., 2008). The atmospheric concentrations of this gas have

* Corresponding author at: Departamento de Química y Tecnología de Alimentos, Escuela Técnica Superior de Ingeniería Agronómica, Alimentaria y de Biosistemas, Universidad Politécnica de Madrid, Ciudad Universitaria, Madrid 28040, Spain.
E-mail address: sandra.garcia@upm.es (S. García-Gutiérrez).

https://doi.org/10.1016/j.geoderma.2023.116424
Received 4 November 2022; Received in revised form 1 March 2023; Accepted 3 March 2023
Available online 10 March 2023

increased approximately 14% since 1940 and have increased substantially in the last decade (Thompson et al., 2019). Nitrous oxide is not only a greenhouse gas (GHG) whose global warming potential is 273 times higher than that of CO_2 (Foster et al., 2021), it also plays an important role in the depletion of stratospheric ozone (Ravishankara et al., 2009).

Nitrification and denitrification are the main microbial processes that lead to the production of N_2O in soils (Butterbach-Bahl et al., 2013; Ussiri and Lal, 2013). These processes are directly affected by the addition of an external N source, although environmental conditions (e.g., climate, soil) and agricultural practices also have an important effect on soil N_2O emissions (Cayuela et al., 2017; IPCC, 2022). Mineral N inputs change the rate of microbial decomposition of soil organic matter (SOM) and crop residues (Elrys et al., 2021), thus increasing the pool of reactive N in the soil. This *priming effect* could also contribute to increased N_2O emissions, as shown in recent laboratory studies using ^{15}N tracing with increases of 19% (Roman-Perez and Hernandez-Ramirez, 2021) and up to 24% (Thilakarathna and Hernandez-Ramirez, 2021) following urea addition.

The integration of crop residues in the N cycle is a key factor for the sustainability of agriculture in semiarid areas (Berhane et al., 2020). Management of C-rich crop residues requires optimum N fertilization to prevent N immobilization (Yansheng et al., 2020), particularly during early crop stages. Crop residues can be incorporated into the soil by conventional tillage (T) or retained on the soil surface through no tillage (NT) practices, a decision that has a key influence on N_2O emissions (Huang et al., 2018). For instance, Abalos et al. (2013) observed that the incorporation of maize stover residue with a high (>70) C:N ratio increased N_2O emissions c. 105%. This could be associated with an enhancement of denitrification due to the interaction between high-C content crop residues with mineral N from dressing fertilization. In non-tilled soils, soil organic C (SOC) accumulates in the topsoil, thus increasing the availability of labile organic C for denitrifiers and mineral N for both nitrifiers and denitrifiers (Shakoor et al., 2021).

One of the most effective strategies for reducing N_2O emissions in fertilized crops is the use of nitrification inhibitors (NIs) (Xia et al., 2017). These products retard the conversion of ammonium (NH_4^+) into hydroxylamine, the first step of nitrification, thereby reducing the amount of nitrate (NO_3^-), which can be easily leached or lost through denitrification (Ruser and Schulz, 2015). Several studies have demonstrated the enhancement of plant N use efficiency and the reduction of N_2O emissions using NIs at a global scale (Qiao et al., 2015). The effectiveness of the NI (3,4-dimethyl-1H-pyrazol-1-yl) succinic acid isomeric mixture (DMPSA) (CA 2,933,591 A1 2015/06/18 Patent) in the mitigation of N_2O emissions has been successfully tested at the field scale (Souza et al., 2021; Cheng et al., 2022; Huérfano et al., 2022). The non-polarity of DMPSA improves the availability of dimethylpyrazole (DMP) in the soil and increases the amount of fertilizer that it can be combined with (e.g., urea, calcium ammonium nitrate, diammonium phosphate) with respect to 3,4-dimethyl pyrazol phosphate (DMPP), another DMP-based NI (Pacholski et al., 2016). It has been observed that the N_2O mitigation of DMPSA is enhanced by NT compared with T under humid rainfed conditions (Corrochano-Monsalve et al., 2020). However, information is scarce regarding the interaction between tillage and inhibitors under semiarid (e.g., dry Mediterranean) conditions. The efficiency of these strategies might be compromised by the emission pattern in semiarid zones, especially in dry seasons when rewetting events can have a large influence on annual N_2O fluxes (Barrat et al., 2021). In addition, there is a trend of increasing aridity as a consequence of decreasing precipitation and increasing temperatures in semiarid Mediterranean areas (Paniagua et al., 2019). Therefore, there is a need to improve the understanding about how these climatological conditions could affect the effectiveness of the above-mentioned strategies, particularly from a mechanistic viewpoint, i.e., exploring the fate of N and the predominant biochemical processes.

Tracing the fate of fertilizer N applied to soil has received attention in recent years because of its close links to N use efficiency and resulting environmental impacts (Sha et al., 2020). Labelled ^{15}N tracing techniques are useful tools that have been widely used not only to monitor the fate of the applied N (Couto-Vázquez and González-Prieto, 2016; Wang et al., 2016; Guardia et al., 2018), but also to accurately quantify the recovery of the fertilizer applied in crop biomass (as well as the relative contribution of endogenous N) and other N pools. A *meta*-analysis of ^{15}N enrichment experimental data reported an average enhancement of 10.5% in crop fertilizer N recovery when NIs such as DCD or DMPP were applied (Sha et al., 2020). However, this study highlighted that there is a lack of knowledge regarding DMPSA application, particularly in rainfed semiarid crops. Moreover, Thilakarathna and Hernandez-Ramirez (2021) found, in a greenhouse experiment, that the inhibition of nitrifier activity affected exogenous fertilizer NH_4^+ and also tended to affect the endogenous NH_4^+ released during the mineralization of SOM and suggested this tendency should be explored using ^{15}N enrichment under field conditions.

In this context, we set up a field experiment aiming to evaluate, using ^{15}N tracing, how tillage management and the use of DMPSA with ammonium nitrate could affect N_2O emissions as well as the fate of synthetic N (soil NH_4^+ and NO_3^-, crop N recovery and soil N retention). With regards to N_2O fluxes, a key objective of this study was to evaluate the efficiency of the DMPSA inhibition potential over both exogenous (fertilizer) and endogenous NH_4^+ as well as the relative contribution of NH_4^+ and NO_3^- to fertilizer-derived N_2O emissions. We hypothesized that i) DMPSA would mitigate N_2O emissions from nitrification of both exogenous and endogenous NH_4^+-N in T and, particularly, in NT and ii) nitrification would be the main process affecting N_2O emissions, as commonly observed in calcareous and low SOM content soils.

2. Materials and methods

2.1. Field microplot experiment

A field experiment using a barley crop (*Hordeum vulgare* L. 'Esterel R1′) was carried out in the National Center of Irrigation Technology "CENTER" in Madrid, Spain (40° 25' 1.31'' N, 3° 29' 45.07'' W). The area has a Mediterranean semiarid climate with high interannual rainfall variability. The soil has been classified as a *Typic xerofluvent* (Soil Survey Staff, 2014) with a silt loam texture in the upper horizon (0–10 cm). The main physicochemical properties of the topsoil before this study are included in Table S1. The barley crop was sown on 17 December 2018 at 200 kg seed ha^{-1}. Rape residues (4492 kg ha^{-1}, with an average C:N ratio of 22.7) were incorporated with a disc harrow and cultivator (in T plots) or left on the soil surface (in NT plots) two months before barley sowing. In the NT plots, glyphosate 36% w/v was applied by spraying before barley seeding.

The experiment consisted of a three-replicate split-plot design with tillage as the main factor (no tillage, NT, and conventional tillage, T) arranged in a randomized block design. The second factor consisted of three fertilizer treatments applied at top-dressing: (1) calcium ammonium nitrate (CAN), (2) CAN with the nitrification inhibitor DMPSA (CAN + DMPSA), and (3) a control without N fertilization (N0). The distribution of subplots (8 m × 8 m) is shown in Fig. S1. Fertilized subplots received 40 kg ha^{-1} of urea at sowing (27 November 2018) and 80 kg N ha^{-1} of CAN at top dressing (14 March 2019).

Additionally, two microplots (1 m × 1 m) were established within every subplot before top dressing fertilization, except in the unfertilized plots (Fig. S1). The microplots consisted of 0.3 m high galvanized sheet iron inserted into the soil to a depth of 0.2 m. Each microplot was amended with 2 L of NH_4NO_3 (AN) solutions enriched with ^{15}N at a N rate of 80 kg N ha^{-1} on 14 March 2019. The solutions consisted of $^{15}NH_4^{14}NO_3$ (^{15}AN) or $^{14}NH_4^{15}NO_3$ ($A^{15}N$) (10 atom % ^{15}N, Campro Scientific) with or without DMPSA and were homogeneously applied with a hand sprayer. The DMPSA inhibitor was provided by EuroChem Agro in a liquid solution and was applied at a rate of 0.8% of the NH_4^+-N

content of the fertilizer. Pests were managed following local practices and irrigation was used on two occasions, on 26 March and 13 May 2019 (20 mm in each event), due to severe drought conditions. The barley was harvested on 13 June 2019. The results presented here are based on the analyses performed in the ^{15}N fertilized microplots and to the N0 subplots after top-dressing N fertilization.

2.2. Nitrous oxide sampling, analysis and flux calculation

Fluxes of N_2O and $^{15}N_2O$ were measured 2–3 times per week during the first month after top-dressing fertilization. Afterwards, the sampling frequency decreased progressively until the end of the field experiment (7 November 2019), including the period after rainfall/irrigation events. The closed chamber technique was used to take gas samples, as described in detail by Guardia et al. (2021). One opaque manual static chamber (12.5 L) was placed in every microplot and control subplot (Fig. S1). Gas samples were taken at times t_0, t_{30} and t_{60} (after 0, 30 and 60 min.) from the headspaces of each chamber using 100 ml syringes fitted with 3-way stopcocks. The concentration of N_2O in the gas samples was determined using an HP-6890 gas chromatograph (GC) equipped with a headspace autoanalyzer (HT3), both from Agilent Technologies (Barcelona, Spain), with a μ-ECD detector. More detailed information is available in Montoya et al. (2021). Fluxes of N_2O were calculated from the slope of the linear regression between concentration and time, and the ratio between chamber volume and soil surface area. Cumulative N_2O-N emissions during the sampling period were estimated by trapezoidal integration of daily fluxes (Cowan et al., 2019).

In the microplots amended with a ^{15}N source, an additional gas sample was obtained at 60 min after closure for $^{15}N_2O$ analyses using preevacuated 12 ml Exetainer gas chromatography vials (Labco Limited, Lampeter, UK). Background gas samples were taken at 0 min in one replicate of each treatment. The vials were sent to a laboratory (Rothamsted Research, North Wyke) to measure the ^{15}N enrichment of N_2O using a TG2 trace gas analyser interfaced to a 20–22 isotope ratio mass spectrometer (both from SerCon Ltd., Crewe, UK). The N_2O in the headspace of the chamber was a mix of atmospheric N_2O at the time of chamber closure and the N_2O emitted from the soil. To obtain the ^{15}N abundances of emitted N_2O (*atom % $^{15}N_{em}$),* the following equation was used:

$$atom\%^{15}N_{em} = (atom\%^{15}N_{mix} \times C_{mix} - atom\%^{15}N_{air} \times C_{air})/C_{em} \quad (1)$$

where '*atom % $^{15}N_{mix}$*' and '*atom % $^{15}N_{air}$*' are the ^{15}N abundances of samples and ambient air (0.362%, the mean natural ^{15}N in our samples), respectively; and 'C_{em}', 'C_{mix}' and 'C_{air}' are the concentrations of N_2O in the headspace (μL N_2O L^{-1}) corresponding to the emission, total sample and atmospheric air (Li et al., 2016) and $C_{mix} = C_{em} + C_{air}$.

The daily N_2O fluxes derived from fertilizer (N_2O-N_{fert}) were calculated according to Guardia et al. (2018):

$$N_2O\text{-}N_{fert} = N_2O\text{-}N \times \left(\frac{ape\ ^{15}N_2O_{em}}{ape\ ^{15}N_{fert}}\right) \quad (2)$$

$$N_2O\text{-}N_{fert} = (N_2O\text{-}N_{15AN}) + (N_2O\text{-}N_{A15N}) \quad (3)$$

where 'N_2O-N' is the daily N_2O emission (mg N m^{-2} d^{-1}). Background $^{15}N_2O$ (0.362%) was subtracted from the *atom % ^{15}Nem* to calculate the atom percent excess (*ape*) of emitted N_2O (*ape $^{15}N_2Oem$*). The ^{15}N *ape* of the fertilizer (*ape $^{15}N_{fert}$*) was calculated by subtracting the mean natural abundance of atmospheric N_2O (0.3663 atom % ^{15}N) from the fertilizer enrichment. The N_2O emissions derived from fertilizer ^{15}AN or $A^{15}N$ were expressed as 'N_2O-N_{15AN}' or 'N_2O-N_{A15N}', respectively.

To obtain the N_2O flux that was derived from soil (N_2O-N_{soil}), the following equation was used:

$$N_2O\text{-}N_{soil} = (N_2O\text{-}N) - (N_2O\text{-}N_{15AN}) - (N_2O\text{-}N_{A15N}) \quad (4)$$

2.3. Soil and plant sampling

Soil samples were collected two to three times per week during the 15 days after fertilization (DAF) using stainless steel cores (5 cm diameter, 10 cm length). Afterwards, the sampling frequency was reduced and soil samples were taken after rain or irrigation events. Fresh soil samples were stored at −20 °C for further mineral N and mineral ^{15}N analyses. In addition, soil was sampled at three depths (0–10, 10–20 and 20–40 cm) at the end of the experiment (7 November 2019) using a stainless steel auger. At the laboratory, fresh soil samples were homogenized and then separated into two subsamples: one subsample was stored at −20 °C for mineral N analysis, and the other subsample was air dried, ground using a ball mill and stored at room temperature for total N and total ^{15}N analysis.

On 13 June 2019, barley plants (shoot and root systems) were sampled using a 0.25 m^2 square, which was placed in the middle of each microplot. The shoot system was cut by sickle at the soil level and was separated into spikes (that were threshed out to obtain the grain) and stems (aboveground biomass). Roots were cleaned with a brush, rinsed thoroughly with tap water (5 min) to separate soil from roots and washed in an ultrasound-assisted bath for 15 min with tap water followed by 5 min with deionized water (García-Gómez et al., 2015). The aboveground biomass and roots were dried to a constant weight at 75 °C, ground using a ball mill and stored until analysis.

2.4. Soil and plant analyses

Water-filled pore space (WFPS) was calculated in fresh soil samples by dividing the volumetric water content (obtained by multiplying the dry-basis gravimetric water content by the bulk density) by the total soil porosity. A particle density of 2.65 g cm^{-3} was assumed for the calculations. The gravimetric water content was determined by oven-drying the soil samples at 105 °C until constant weight.

Mineral N (NH_4^+-N and NO_3^--N) was extracted from fresh homogenized soil samples using 1 M KCl (1:6.25, w:v). Soil extracts were filtered using a) Filter-Lab 1250 cellulose filters previously washed with 1 M KCl to analyse $^{15}NH_4^+$-N and $^{15}NO_3^-$-N; and b) 0.45 μm cellulose filters (Teknokroma) to measure NH_4^+-N and NO_3^--N concentrations by automated colorimetric determination using a flow injection analyser (FIAS 400 Perking Elmer) provided with a UV–vis spectrophotometer detector. Both soil extracts were stored at −20 °C until analysis.

The $^{15}NH_4^+$ and $^{15}NO_3^-$ in the soil extracts were sequentially transferred in the form of NH_3 to an acidified cellulose disc using the microdiffusion technique described by Hart and Stark (1994) with some modifications. Detailed information can be found in the supplementary material. Total N and ^{15}N in discs from both diffusions of each extract were analysed by isotope ratio mass spectrometry (IRMS) at the Interdepartmental Investigation Service at Universidad Autónoma of Madrid (SIdI-UAM) through combustion of samples using an elemental analyser Thermo 1112 Flash HT hyphenated to an IRMS Thermo Delta V Advantage.

To determine how much NH_4^+–N or NO_3^-–N in the soil came from the fertilizer or from the soil, the following equations were used:

$$NH_4^+\text{-}N_{15AN}\ (or\ NH_4^+\text{-}N_{A15N}) = Total\ NH_4^+\text{-}N \times \left(\frac{ape\ ^{15}N_{filter}}{ape\ ^{15}N_{fert}}\right) \quad (5)$$

$$NH_4^+\text{-}N_{soil} = Total\ NH_4^+\text{-}N - (NH_4^+\text{-}N_{15AN}) - (NH_4^+\text{-}N_{A15N}) \quad (6)$$

where 'NH_4^+-N_{15AN}' (or NH_4^+-N_{A15N}) is the NH_4^+-N in the soil that was derived from ^{15}AN or $A^{15}N$ fertilizer (kg N ha^{-1}), respectively. The '*Total NH_4^+-N*' is the concentration of NH_4^+-N total in soil obtained from the results of the first microdiffusion. The '*ape $^{15}N_{filter}$*' was obtained by subtracting the background atom % ^{15}N (0.3663 atom % ^{15}N) from the atom % ^{15}N in the filters of the first microdiffusion. Similar calculations were carried out to obtain 'NO_3^--N_{15AN}', 'NO_3^--N_{A15N}', and 'NO_3^--N_{soil}'

using the results obtained in the second microdiffusion. For these calculations, '*Total NO_3^--N*' is the concentration of NO_3^--N in soil obtained by the results from the second microdiffusion.

The gross N mineralization rate (i.e., an indicator of the amount of organic-N that is mineralized to NH_4^+ by ammonifiers) was estimated from the rate of dilution of ^{15}N enrichment in the NH_4^+ pool and from the change in the total NH_4^+ pool size, following the equations of Kirkham and Bartholomew (1954). The gross N nitrification rate was calculated from the equations of Ruppel et al. (2006).

The total N and ^{15}N contents in the soil depth samples and in the plant material were analysed by IRMS at SIdI-UAM. Calculations of the contribution of each labelled fertilizer (^{15}AN o $A^{15}N$) to the N uptake by plants and to the N retention in soil were calculated according to Guardia et al. (2018):

$$plant\_N_{15AN}(or\ plant\_N_{A15N}) = plant\_TN \times \frac{ape^{15}N_{planr}}{ape^{15}N_{fert}} \quad (7)$$

$$plant\_N_{fert} = plant\_N_{15AN} + plant\_N_{A15N} \quad (8)$$

where '*plant_N_{15AN}*' (or '*plant_N_{A15N}*') is the N in each part of barley plant that was derived from ^{15}AN or $A^{15}N$ fertilizer, respectively. '*plant_TN*' is the total N uptake in the corresponding part of the plant (kg N ha^{-1}), obtained by multiplying the N % in the plant by the crop yield (kg ha^{-1}) × 100. The '*ape $^{15}N_{plant}$*' was obtained by subtracting the background atom % ^{15}N (0.3663 atom % ^{15}N) from the atom % ^{15}N in the plant sample.

Plant N derived from soil (*plant_N_{soil}*) was calculated as follows:

$$plant\_N_{soil} = plant\_TN - plant\_N_{fert} \quad (9)$$

This calculation assumes that the plants did not discriminate between ^{15}N and ^{14}N sources of fertilizer N.

Calculations for '*soil_N_{fert}*', '*soil_N_{15AN}*', '*soil_N_{A15N}*', '*soil_N_{soil}*' and '*ape_{soil}*' at the three different soil sampling depths were similar to those for '*plant_N*'. '*Soil_TN*' is the total N at the corresponding soil depth, obtained as follows:

$$soil\_TN = (soil\_N\% \times bulk\ density \times N\ fertilization\ rate)/100 \quad (10)$$

The N fertilizer recovery (%) in plants and soil was calculated as follows:

$$plant\_N_{recovery}(or\ soil\_N_{retention}) = \frac{plant\_N_{fert}(or\ soil\_N_{fert})}{N\ fertilization\ rate} \times 100 \quad (11)$$

2.5. Statistical analyses

Data analysis was performed using Statgraphics® Centurion 19 software. Data distribution normality and variance uniformity were verified by the Shapiro-Wilk and Levene's test, respectively, and inverse or log transformations were applied before analysis when necessary. Two-way ANOVAs were conducted to analyse the significant differences in tillage and fertilization factors (and in the interaction between them). The LSD test at $P < 0.05$ was used for multiple comparisons between means. To analyse the differences between N derived from ^{15}AN and N derived from $A^{15}N$, an additional factor (^{15}N labelling, ^{15}AN or $A^{15}N$) was included in the general linear model for the ANOVA, in addition to tillage and fertilization (i.e., split-split-plot).

3. Results

3.1. Environmental conditions

From top-dressing fertilization (14 March) to harvest (13 June), the accumulated rainfall was 96 mm (136 mm including irrigation events). This accumulated rainfall was lower than the 15-year average in the area (118 mm). A remarkable rainfall event (35.6 mm) took place during the postharvest period (26 August) after several weeks of drought and high air and soil temperatures (Fig. 1a). Throughout the experimental period (from March to November), the minimum and maximum soil temperatures (10 cm depth) were 10.9 °C and 25.8 °C, respectively, with a mean temperature of 19.3 °C (Fig. 1a).

The WFPS (Fig. 1b) ranged from 10.2% to 62.6% during the preharvest period, with values below 30% in the upper soil layer most of this time. It was only above 45% at the end of April and in mid-May as a consequence of rainfall or irrigation events. During summer, the soil remained dry (WFPS <20%); however, after the rainfall event on 26 August, the WFPS increased from 10.2% to 44.7%. No significant differences in WFPS were found between the tillage systems.

3.2. Mineral N, ^{15}N-NH_4^+ and ^{15}N-NO_3^- in soil

The soil NH_4^+ concentration was <10 mg NH_4^+-N kg^{-1} the day before top-dressing fertilizer application (13 March) in all plots, without significant differences between tillage management or fertilization treatments (Fig. S2a). Until harvest, the mean NH_4^+ concentrations in the soil were in the following order: AN + DMPSA > AN > N0, with no effect of tillage (Table 1).

The results of NH_4^+-N obtained from the microdiffusions in soil extracts from 14 March to 4 April are included in Fig. 2, showing that 75.4% (on average) of NH_4^+-N was derived from top-dressing N fertilization (Table 2). Significant differences in fertilization treatments were observed only for NH_4^+-N_{15AN}, which was higher in AN + DMPSA (by 75.1% on average) with respect to AN.

The soil NO_3^- concentration ranged from 10.3±3.9 to 52.3±5.8 mg NO_3^--N kg^{-1} the day before top-dressing fertilizer application (13 March), with a significantly higher concentration in the T plots than in the NT plots (Fig. S2b). The mean NO_3^- concentration in the T plots was double that of the NT plots in the preharvest period (Table 1). However, DMPSA did not affect the NO_3^- concentration with respect to AN-only, and both fertilized treatments led to higher values compared with N0. At the end of the experiment, the NO_3^- concentration increased with depth, and the highest values were reported in the T_AN treatment (Table S2).

During the period from 14 March to 4 April, significant differences in soil management were observed for NO_3^--N_{soil} (Fig. 3), which was on average 2.5 times higher in T than in NT (Table 2). This was not observed for NO_3^--N_{fert} (neither for ^{15}AN nor for $A^{15}N$). On average, N fertilization (^{15}AN + $A^{15}N$) contributed to 35.5% and 52.9% of the NO_3^- concentrations in the soil in T and NT, respectively. The NO_3^--N_{15AN} concentrations were lower than those of NO_3^--N_{A15N} (Fig. 3, Table 2).

The mean gross mineralization rate during the sampling period was 1.6 mg N kg^{-1} d^{-1} and no differences between treatments were observed (Table S3). In general, the largest values of gross mineralization rates were obtained during the first 24 h, ranging from 1.1 mg N kg^{-1} d^{-1} (T_AN + DMPSA) to 5.2 mg N kg^{-1} d^{-1} (NT_AN + DMPSA) (data not shown). The mean gross nitrification rate was 0.7 mg N kg^{-1} d^{-1}, and values were numerically higher in NT and in AN than in T and AN + DMPSA, respectively (Table S3).

3.3. N_2O and $^{15}N_2O$ emissions

3.3.1. Emissions after top dressing fertilization (preharvest period)

The main N_2O emission peaks occurred immediately after the second irrigation event (i.e., 61 days after N application), reaching 0.49 mg N m^{-2} d^{-1} in NT_AN (Fig. 4a). Cumulative N_2O fluxes before harvest were in the following order: AN > AN + DMPSA > N0 (Fig. 5), with the emissions from AN + DMPSA being 60% lower than those from AN. Most of the N_2O emitted (85%, on average) during this period was derived from the endogenous N of the soil (Fig. S3), regardless of tillage or fertilizer treatments (Table 3). The use of DMPSA abated N_2O-N_{15AN} (by 74%), N_2O-N_{A15N} (by 46%) and N_2O-N_{soil} (by 60%) emissions compared with AN, regardless of tillage management ($P < 0.05$). The relative

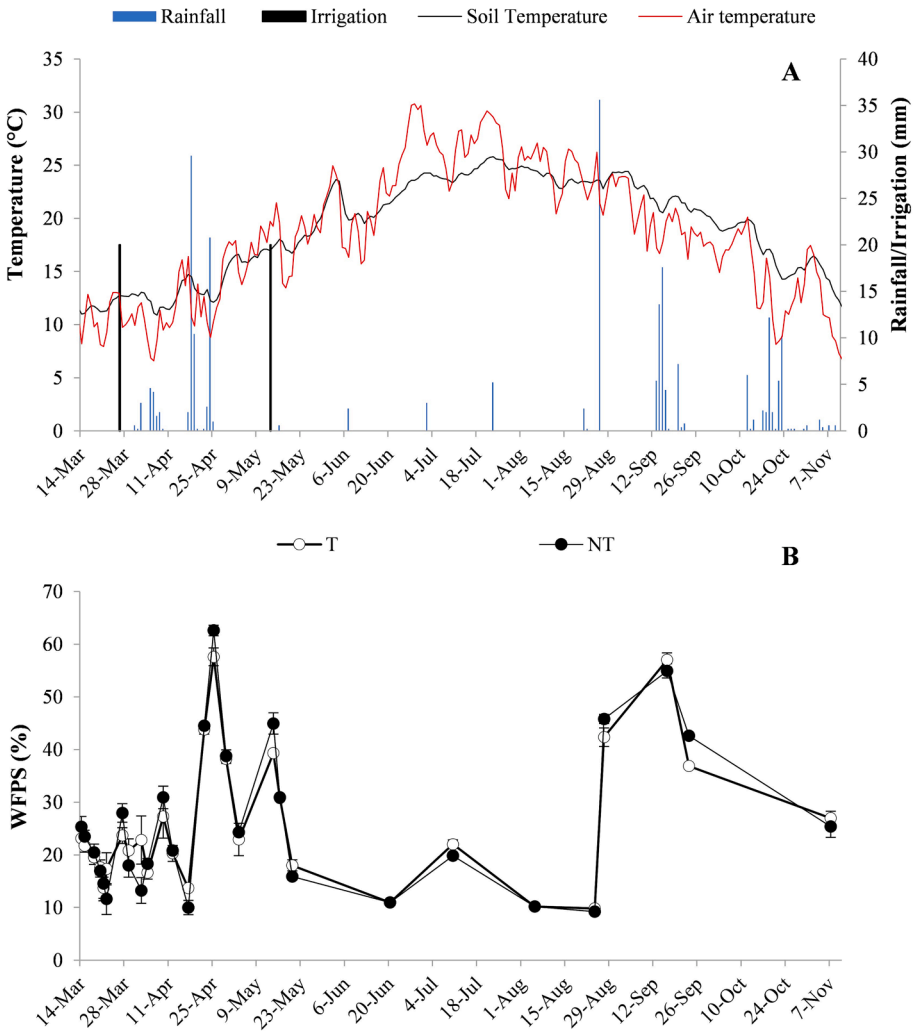

Fig. 1. A) Daily mean air and soil (10 cm depth) temperature and daily rainfall during the experimental period (14 March to 9 November 2019). Two irrigation events (black bars, 20 mm each) were performed on 26 March and 13 May. **B)** Evolution of soil WFPS (0–10 cm) in the different tillage (conventional tillage, T, no tillage, NT) plots. The black arrows denote irrigation events (26 March and 13 May). Vertical bars indicate standard errors of the means.

Table 1
Mean soil mineral N (NH_4^+-N and NO_3^--N) concentrations in the preharvest period.

	NH_4^+ (mg N kg soil^{-1})	NO_3^- (mg N kg soil^{-1})
Tillage		
T	8.16	48.9 b
NT	5.90	24.4 a
S.E.	0.76	2.2
P value	0.171	0.016
Fertilizer		
N0	2.73 a	19.8 a
AN	7.71 b	41.8 b
AN + DMPSA	10.65 c	48.4 b
S.E.	0.95	2.4
P value	0.000	0.000
Tillage × Fertilizer		
P value	0.711	0.179

Different letters within columns indicate significant differences within each effect according to the LSD test at $P < 0.05$. S.E.: Standard error of the mean.

contribution of exogenous NO_3^- was lower than that of exogenous NH_4^+ or endogenous N, ranging from 4% in T_AN to 9% in NT_AN + DMPSA (Table 3).

3.3.2. *Emissions during the postharvest period*

Nitrous oxide emissions were negligible when daily effective rainfall was below 5 mm. However, after the rainfall event at the end of August (Fig. 1a), N_2O fluxes peaked (Fig. 4b). The N_2O emissions during this summer peak were similar for all the tillage × fertilizer combinations except for the NT_N0 treatment, which had the lowest value ($P < 0.05$). The N_2O emitted during that pulse had a pivotal influence on total cumulative fluxes, leading to total emissions from AN to be numerically, but not statistically, higher than those from AN + DMPSA (Fig. 5). In contrast to the preharvest period, N_2O-N_{15AN} emissions after harvest and until the end of the experiment were significantly lower than those derived from $A^{15}N$ (Table 3). Like during the crop period, most N_2O emissions were derived from the soil (i.e., 95%, on average).

3.4. *Total N and ^{15}N in barley plants*

The mean total N in grain, aboveground biomass and root biomass of barley plants was 2.3%, 1.1% and 1.4%, respectively, with no significant differences between any of the tillage-fertilizer combinations (Table S4). Plant N uptake was increased in AN + DMPSA, with respect to AN, in

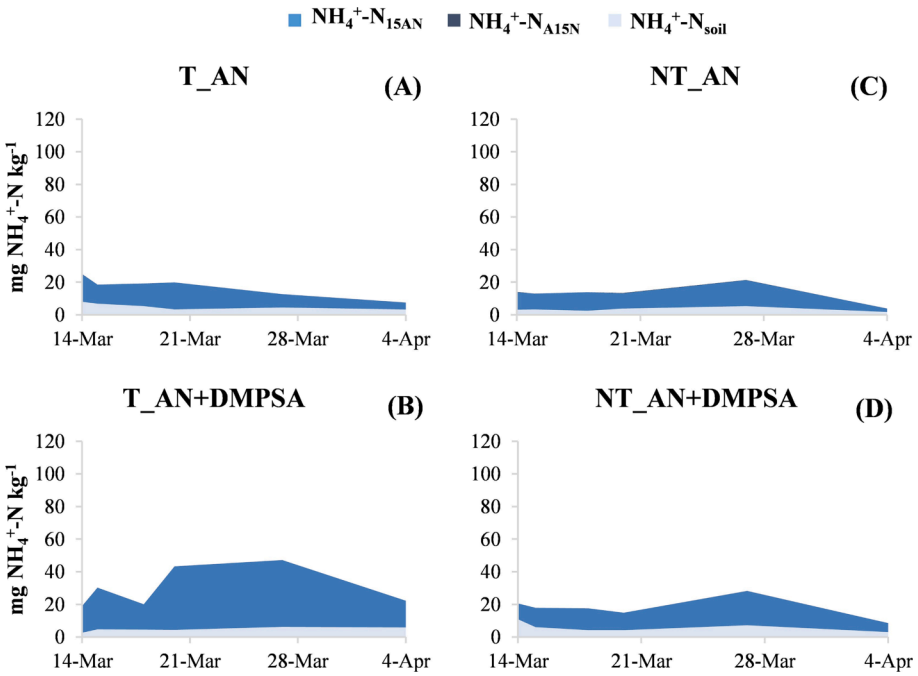

Fig. 2. Evolution of NH_4^+-N concentration derived from soil (NH_4^+-N_{soil}), from $^{15}NH_4NO_3$ (NH_4^+-N_{15AN}) and from $NH_4^{15}NO_3$ (NH_4^+-N_{A15N}) during 21 days following top dressing fertilization (14 March) in the different soil tillage (conventional tillage, T, no tillage, NT) and fertilizer (NH_4NO_3, AN, NH_4NO_3 with DMPSA, AN + DMPSA) treatments. T_AN (**A**), T_AN + DMPSA (**B**), NT_AN (**C**) and NT_AN + DMPSA (**D**).

Table 2
Mean values obtained from microdiffusions (from 14 March to 4 April) of mineral N derived from $^{15}NH_4NO_3$ (NH_4^+-N_{15AN} and NO_3^--N_{15AN}), derived from $NH_4^{15}NO_3$ (NH_4^+-N_{A15N} and NO_3^--N_{A15N}), and from the soil (NH_4^+-N_{soil} and NO_3^--N_{soil}) (mg N kg^{-1}) in the different soil tillage (conventional tillage, T, no tillage, NT) and fertilizer (NH_4NO_3, AN, NH_4NO_3 with DMPSA, AN + DMPSA) treatments. Data in parentheses indicate the % with respect to total NH_4^+-N or NO_3^--N.

	NH_4^+-N_{15AN}	NH_4^+-N_{A15N}	NH_4^+-N_{soil}	NO_3^--N_{15AN}	NO_3^--N_{A15N}	NO_3^--N_{soil}
Tillage						
T	18.8 (79.1)	0.002 (0.0)	4.97 (20.9)	2.52 (3.3)	24.7 (32.2)	49.6 (64.5) b
NT	11.3 (69.9)	0.013 (0.1)	4.85 (30.1)	2.99 (7.2)	19.0 (45.7)	19.6 (47.1) a
S.E.	2.2	0.003	0.11	0.09	1.8	3.9
P value	0.227	0.118	0.549	0.062	0.157	0.032
Fertilizer						
AN	10.9 (71.9) a	0.003 (0.0)	4.28 (28.1)	2.64 (4.6)	23.1 (40.6)	31.1 (54.8)
AN + DMPSA	19.1 (77.5) b	0.012 (0.0)	5.54 (22.5)	2.86 (4.7)	20.6 (33.6)	38.0 (61.8)
S.E.	1.2	0.003	0.81	0.27	3.3	3.3
P value	0.033	0.089	0.332	0.597	0.627	0.238
Tillage × Fertilizer						
P value	0.212	0.251	0.200	0.349	0.433	0.479

Different letters within columns indicate significant differences within each effect according to the LSD test at $P < 0.05$. S.E.: Standard error of the mean.

grain (by 9% on average), biomass (by 24% on average) and roots (by 11% on average), although these increases were only significant for NT plots (Table S4).

Regarding ^{15}N analyses, differences were observed in the % ^{15}N in grain, with higher values obtained in barley plants grown in T compared with those from NT plots and in plants fertilized with $A^{15}N$ versus ^{15}AN (Table 4). The use of DMPSA affected plant_N_{soil}, which was higher in AN + DMPSA than in AN in grain (by 14.8%, $P < 0.05$) and by 21.1% and 13.5% in biomass and roots, respectively ($0.05 < P < 0.10$). Generally, no differences in the plant_N_{fert} were observed between tillage or fertilization treatments, except for the higher values in NT than in T for biomass (21% increment, $P < 0.05$) (Table 4). Accordingly, NT plots had higher N recovery in aboveground biomass (Table S5) and tended to have larger total recovery in plants with respect to T. On average, 22% of the N applied at top dressing fertilization was recovered in barley plants, with no significant effect of tillage or DMPSA addition. Values corresponding to plant_N_{A15N} were statistically higher than those from plant_N_{15AN} for all components of barley yield (Table 4).

3.5. Retention of ^{15}N in soil

At the end of the experiment, soil_N_{15AN} was mainly retained in the upper soil layer, showing higher values with the use of DMPSA (9.7 kg N ha^{-1}) compared with AN (4.9 kg N ha^{-1}, Fig. 6). Tillage management did not affect soil_N_{15AN} or soil_N_{A15N} in the upper layer. However, soil_N_{A15N} at deeper soil layers (10–20 cm and 20–40 cm) was higher in the T plots than in the NT plots, while no differences were observed between fertilization treatments (Fig. 6). Total soil N retention ranged from 28.6% (in NT_AN) to 49.5% of synthetic N applied (in T_AN + DMPSA) without significant differences between treatments (Table S6). On average, the non-accounted N reached 41%.

4. Discussion

There is a remarkable inter-annual meteorological variability in semi-arid Mediterranean croplands. However, the frequency of cropping campaigns with low cumulative precipitation is increasing in these areas (Paniagua et al., 2019). The results of our study were obtained in a dry cropping period (see section 3.1). However, half of the campaigns during the last 15-years reported even lower cumulative rainfall in the March-July period than in our experiment (considering the irrigation events) (Table S7). These meteorological conditions affect the environmental impacts of N fertilization and N dynamics that should be explored mechanistically. Field experiments shed light on N fate, N

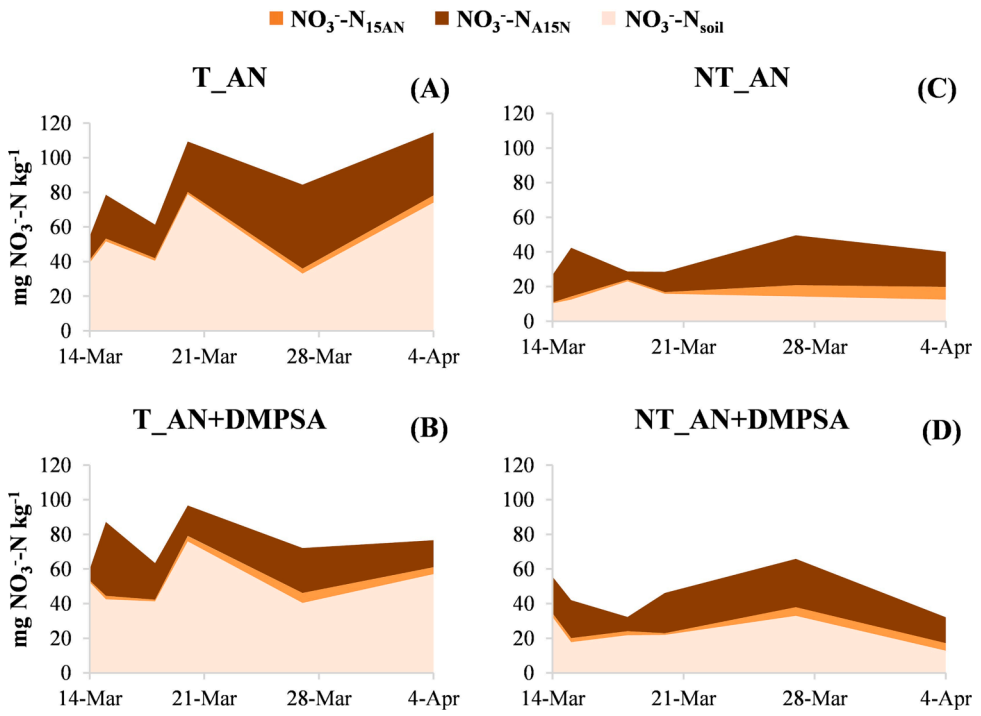

Fig. 3. Evolution of NO_3^--N concentration derived from soil (NO_3^--N_{soil}), from $^{15}NH_4NO_3$ (NO_3^--N_{15AN}) and from $NH_4^{15}NO_3$ (NO_3^--N_{A15N}) during 21 days following top dressing fertilization (14 March) in the different soil tillage (conventional tillage, T, no tillage, NT) and fertilizer (NH_4NO_3, AN, NH_4NO_3 with DMPSA, AN + DMPSA) treatments. T_AN (**A**), T_AN + DMPSA (**B**), NT_AN (**C**) and NT_AN + DMPSA (**D**).

cycling and the potential benefits of recommended agricultural practices. Under the conditions of our study, we can conclude that i) dry seasons could decrease N_2O losses after fertilization but lead to critical peaks after rewetting, thus limiting the effectiveness of mitigation strategies; ii) nitrification inhibitors modulate the nitrification process from both fertilizer-N and endogenous-N (which is the main contributor to plant uptake), affecting soil residual N at the end of the cropping period; and iii) the effect of no tillage on N_2O fluxes and soil and plant recovery could be mainly related to plant N acquisition.

4.1. Soil mineral N during the preharvest period

Crop residue management practices affected NO_3^--N concentrations in the soil (0–10 cm depth), with higher values for the tilled plots than in the non-tilled plots (Table 1). Similar results were reported previously under rainfed Mediterranean conditions (Plaza-Bonilla et al., 2014; Corrochano-Monsalve et al., 2020). This could be related to the higher crop density and early crop development observed in the non-tilled plots that could have enhanced crop N acquisition, thus reducing the soil N pool. Improved crop development using conservation tillage management under Mediterranean conditions has been previously reported by Morell et al. (2011).

The effectiveness of DMPSA in inhibiting NH_4^+ oxidation has been previously reported in several studies under similar climatic conditions (Volpi et al., 2017; Guardia et al., 2021). Our results confirm this with an increase of 39% in the average soil NH_4^+-N in AN + DMPSA compared with AN during the preharvest period (Table 1). These results are in agreement with the well-known effect of NIs at a global scale (Qiao et al., 2015) and are related to the increase in the amount of NH_4^+-N derived from the fertilizer (Table 2). The reduced effect of DMPSA on non-tilled plots (in comparison with conventional tillage) could be associated with the potentially higher NH_4^+ uptake in NT plots (see Section 3.4) or with the generally higher N losses through volatilization in non-tilled than in tilled soils (Pinheiro et al., 2018).

The decrease in NH_4^+-N_{15AN} in fertilized plots coinciding with an increase in the NO_3^--N_{15AN} concentrations during the 3 following weeks after N fertilization (Fig. 2 and Fig. 3, respectively) could have been the result of nitrification (Zhu et al., 2019; He et al., 2020), considering the low WFPS values (Pilegaard, 2013). The gross nitrification rates reported in the present study (0.7 mg N kg^{-1} d^{-1} on average, Table S3) are of the same order of magnitude as those obtained previously under field conditions, e.g., 0.3 mg N kg^{-1} d^{-1} in a neutral pH soil in England (Geens et al., 1991) and 0.8 mg N kg^{-1} d^{-1} in a calcareous soil in England (Unkovich et al., 1998). As mentioned above, DMPSA effectively inhibited NH_4^+ oxidation. Thus, higher gross nitrification rates in AN compared with AN + DMPSA would be expected. We observed high variability in the gross nitrification rates (0.89±0.33 and 0.60±0.10 mg N kg^{-1} d^{-1} in AN and AN + DMPSA respectively, Table S3), thus masking the effect of DMPSA at a statistical level. However, despite this variability, we observed a decrease of 32% in the AN + DMPSA treatment with respect AN. These results highlight the challenges when developing ^{15}N tracing studies under field conditions, such as ensuring the uniform distribution of the applied ^{15}N-label throughout the soil (Murphy et al., 2003), the presence of plants that are known to influence gross N transformation rates (Inselsbacher et al., 2013; He et al., 2020) or adverse meteorological conditions or unaccounted for N losses via NH_3 volatilization (Pan et al., 2016), which should be taken into account in future studies to better understand the N dynamics in agricultural fields.

Our values of gross mineralization (1.6 mg N kg^{-1} d^{-1} on average, Table S3) were lower than those reported by Geens et al. (1991) (2.4 kg N ha^{-1} d^{-1}), Unkovich et al. (1998) (3.6 mg N kg^{-1} d^{-1}), Ruppel at al. (2006) (3.7 mg N kg^{-1} d^{-1}) and Harty et al. (2017) (5.2 mg N kg^{-1} d^{-1}). Our lower values could be explained by the low organic matter content of this soil (<2%) and the dry conditions during the two weeks following fertilization (Fig. 1a and b).

4.2. N_2O emissions

4.2.1. Emissions after top dressing fertilization (preharvest period)

The scarce precipitation during the experiment (Fig. 1a) was likely a key driver of the low N_2O emissions after N top dressing fertilization

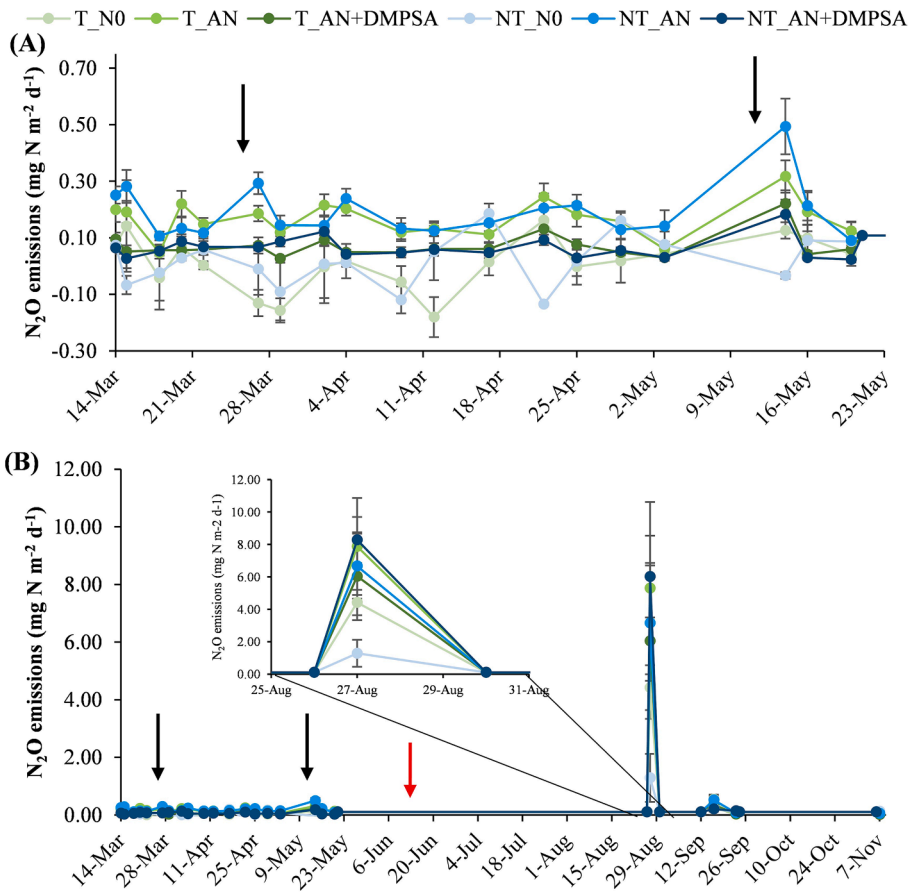

Fig. 4. Daily N_2O emissions in the preharvest period **(A)** and during the whole experimental period **(B)** for the different soil tillage (conventional tillage, T, no tillage, NT) and fertilizer (unfertilized N control, N0, NH_4NO_3, AN, NH_4NO_3 with DMPSA, AN + DMPSA) treatments. The black arrows denote irrigation events. The red arrow denotes the day of barley harvest. Vertical lines indicate standard errors of the means.

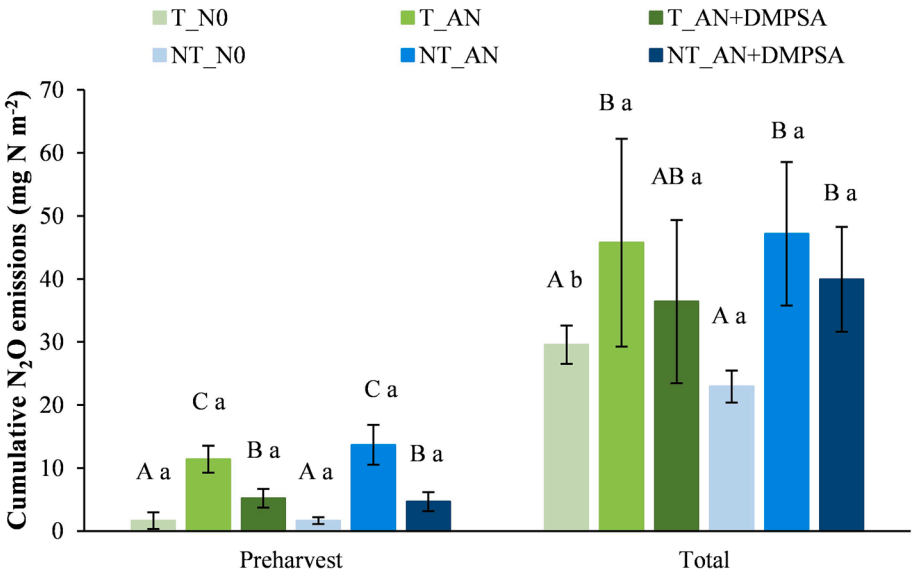

Fig. 5. Cumulative N_2O emissions at preharvest and total N_2O emissions at the end of the experiment (i.e., preharvest + postharvest) in the different soil tillage (conventional tillage, T, no tillage, NT) and fertilizer (unfertilized N control, N0, NH_4NO_3, AN, NH_4NO_3 with DMPSA, AN + DMPSA) treatments. Vertical lines indicate standard errors of the means. Different capital letters indicate differences ($P < 0.05$) between fertilizer treatments within each tillage treatment. Different lowercase letters indicate significant differences ($P < 0.05$) between tillage treatments within each fertilizer treatment.

(Fig. 4a, Table 3), with lower values than those reported in other studies in rainfed crops under semiarid Mediterranean conditions, e.g., 9 – 80 mg N m^{-2} in Guardia et al. (2021) or 20–124 mg N m^{-2} in Montoya et al. (2021), the latter including the postharvest period. Dry conditions, low soil moisture and organic C content, and calcareous soils are all factors that are expected to lead to low N_2O fluxes (Aguilera et al., 2013; Cayuela et al., 2017). Moreover, dry conditions are expected to favour conservation over conventional tillage with regards to crop development and plant recovery (Morell et al., 2011), thus changing soil N availability and N_2O emission dynamics (Huang et al., 2018) and, therefore, modifying the relevance of the post-harvest N_2O emission peaks after rewetting (Barrat et al., 2021).

Table 3
Preharvest and postharvest cumulative N_2O-N emissions derived from $^{15}NH_4NO_3$ (N_2O-N_{15AN}), $NH_4^{15}NO_3$ (N_2O-N_{A15N}) and from the soil (N_2O-N_{soil}) in the different soil tillage (conventional tillage, T, no tillage, NT) and fertilizer (NH_4NO_3, AN, NH_4NO_3 with DMPSA, AN + DMPSA) treatments.

	N_2O (mg N m^{-2})					
	Preharvest			Postharvest		
	N_2O-N_{15AN}	N_2O-N_{A15N}	N_2O-N_{soil}	N_2O-N_{15AN}	N_2O-N_{A15N}	N_2O-N_{soil}
Tillage						
T	0.70	0.37	7.13	0.30 a	1.23	31.4
NT	1.08	0.49	7.55	0.74 b	0.91	32.7
S.E.	0.22	0.09	0.41	0.07	0.39	2.2
***P* value**	0.342	0.448	0.539	0.046	0.622	0.653
Fertilizer						
AN	1.41 b	0.56 b	10.5 b	0.52	1.10	32.3
AN + DMPSA	0.37 a	0.30 a	4.22 a	0.53	1.03	31.8
S.E.	0.26	0.05	0.41	0.12	0.25	2.1
***P* value**	0.018	0.016	0.000	0.974	0.841	0.640
Tillage × Fertilizer						
T_AN	0.87	0.57	9.84	0.32	1.31	32.8
T_AN + DMPSA	0.53	0.18	4.42	0.29	1.14	29.9
NT_AN	1.95	0.55	11.1	0.72	0.89	31.9
NT_AN + DMPSA	0.21	0.43	4.02	0.77	0.92	33.6
S.E.	0.37	0.06	0.58	0.17	0.35	3.0
***P* value**	0.071	0.110	0.231	0.842	0.783	0.526

Different letters within columns indicate significant differences within each effect according to the LSD test at $P < 0.05$. S.E.: Standard error of the mean.

The low WFPS in the upper soil layer reported after top dressing fertilization (Fig. 1b) could have favoured top-dressing fertilizer retention in this layer. Most N_2O emissions were derived from endogenous soil N (Table 3, Fig. S3), which could be related to the previously reported priming effect that occurs after synthetic N addition (Schleusner et al., 2018; Thilakarathna and Hernandez-Ramirez, 2021). These endogenous N_2O emissions could also be derived from the N remaining from the fertilizer application at sowing. When focusing on N_2O emissions derived from dressing N fertilization, the N_2O coming from NH_4^+ was higher than that from NO_3^- (Table 3), suggesting that nitrification (*per se* or coupled with denitrification) was a relevant process for N_2O emissions during this period, as usually observed in Mediterranean cropping systems (Aguilera et al., 2013) and in agreement with our second hypothesis.

The effectiveness of DMPSA in reducing N_2O emissions until harvest was demonstrated with the 61% lower cumulative fluxes reported in the microplots that received DMPSA (Table 3). In addition to the well-known effect of DMPSA inhibiting nitrification from fertilizer NH_4^+-N (Huérfano et al., 2016; Torralbo et al., 2017; Montoya et al., 2021; Guzman-Bustamante et al., 2022), we observed that DMPSA also mitigated the N_2O emissions derived from the endogenous N in both tillage systems, thus supporting our first hypothesis. Our results suggest that DMPSA can move within the soil profile, as seen for DMPP (another DMP-based NI) from another study (Marsden et al., 2016), and inhibit the oxidation of the remaining NH_4^+ from basal fertilization and SOM mineralization, which had rates that were higher than those of nitrification. Besides the understandable effect of DMPSA on the N_2O coming from endogenous or exogenous NH_4^+, a significant effect of the inhibitor was also observed in N_2O derived from fertilizer NO_3^--N (Table 3), as reported by Guardia et al. (2018), who also used single-labelled ammonium nitrate (i.e., ^{15}AN and A^{15}N) but in a maize crop. It has been demonstrated that soils with rapid nitrification rates (e.g., calcareous or alkaline) promote oxygen depletion and nitrite (NO_2^-) accumulation, thus stimulating denitrification and increasing the N_2O:N_2 ratio

Table 4
Plant ^{15}N percentage (% ^{15}N), plant N derived from fertilizer (Plant_N_{fert}), plant N derived from soil (Plant_N_{soil}) and plant N recovery in the different soil tillage (conventional tillage, T, no tillage, NT) and fertilizer (NH_4NO_3, AN, NH_4NO_3 with DMPSA, AN + DMPSA) treatments and in the different ^{15}N labelling treatments ($^{15}NH_4NO_3$, ^{15}AN, $NH_4^{15}NO_3$, A^{15}N).

	% ^{15}N			Plant_N_{fert} (kg N ha^{-1})			Plant_N_{soil} (kg N ha^{-1})			N recovery (%)
	Grain	Biomass	Root	Grain	Biomass	Root	Grain	Biomass	Root	Plant
Tillage										
T	1.49 b	1.39	1.10	9.74	5.95 a	0.31	32.5	22.0	1.69	20.0
NT	1.36 a	1.32	1.11	12.3	7.53 b	0.40	48.7	30.8	2.27	25.3
S.E.	0.02	0.05	0.03	1.34	0.08	0.03	4.9	1.8	0.18	1.7
P value	0.046	0.393	0.9499	0.309	0.005	0.182	0.144	0.068	0.158	0.161
Fertilizer										
AN	1.50	1.42	1.16	11.5	6.68	0.36	37.8 a	23.8	1.86	23.2
AN + DMPSA	1.34	1.29	1.05	10.5	6.80	0.35	43.4 b	29.0	2.11	22.1
S.E.	0.13	0.12	0.08	0.62	0.34	0.02	1.3	1.9	0.08	1.2
P value	0.391	0.414	0.326	0.306	0.819	0.576	0.008	0.056	0.097	0.533
Tillage × Fertilizer										
T_AN	1.53	1.42	1.14	10.4	6.06	0.33	32.6 Aa	21.3	1.70	21.0
T_AN + DMPSA	1.45	1.36	1.07	9.05	5.84	0.29	32.3 Aa	22.7	1.69	19.0
NT_AN	1.75	1.42	1.18	12.6	7.30	0.40	43.0 Ab	26.3	2.01	25.4
NT_AN + DMPSA	1.24	1.21	1.03	12.0	7.76	0.40	54.4 Bb	35.2	2.52	25.2
S.E.	0.18	0.17	0.11	0.85	0.48	0.03	1.8	2.7	0.12	1.6
P value	0.668	0.631	0.715	0.689	0.519	0.472	0.005	0.197	0.084	0.597
Label										
^{15}AN	1.09 a	1.04 a	0.90 a	3.89 a	2.10 a	0.12 a				
A^{15}N	1.76 b	1.67 b	1.31 b	7.13 b	4.64 b	0.23 b				
S.E.	0.05	0.04	0.03	0.23	0.16	0.01				
P value	0.000	0.000	0.000	0.000	0.000	0.000				

Different letters within columns indicate significant differences within each effect according to the LSD test at $P < 0.05$. Different capital letters in the "Tillage × Fertilizer" interaction indicate significant differences between fertilizers within each tillage system, while different lowercase letters indicate significant differences between tillage systems within each fertilization treatment. S.E.: Standard error of the mean.

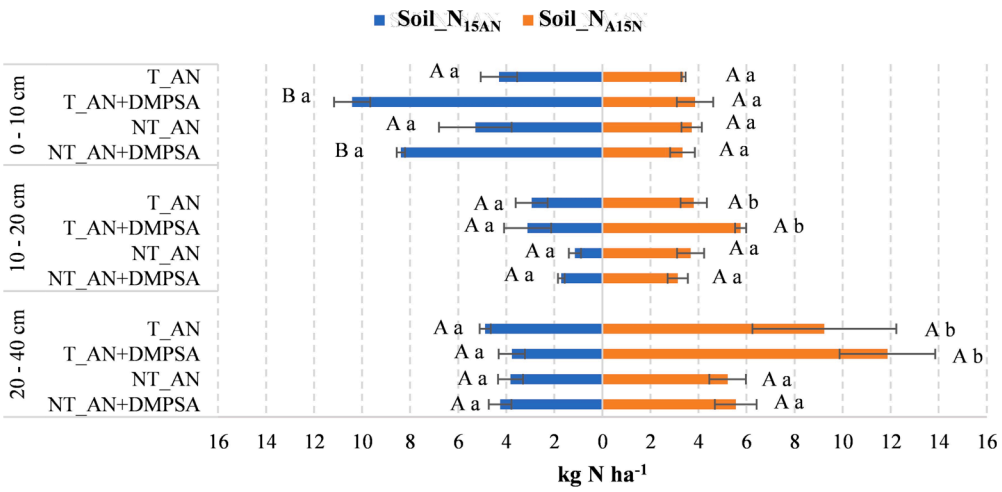

Fig. 6. Average soil N derived from ^{15}AN (Soil_N_{15AN}) and derived from A^{15}N (Soil_N_{A15N}) at 0–10 cm, 10–20 cm and 20–40 cm depths at the end of the experiment (7 November) in the different soil tillage (conventional tillage, T, no tillage, NT) and fertilizer (NH_4NO_3, AN, NH_4NO_3 with DMPSA, AN + DMPSA) treatments. Horizontal lines indicate standard errors. Different capital letters indicate differences ($P < 0.05$) between fertilizers within each soil management system, while different lowercase letters indicate significant differences ($P < 0.05$) between soil management within each fertilization treatment.

(Petersen et al., 1996; Li et al., 2023). Therefore, the inhibiting effect of DMPSA is also expected to detrimentally affect denitrification rates and the amount of N_2O derived from A^{15}N. A clear effect of nitrification inhibitors such as DMPP or DMPSA on denitrifying microorganisms has also been observed by e.g., Torralbo et al. (2017) or Barrena et al. (2017), decreasing the abundance of genes involved in the stepwise reduction of NO_3^- to NO_2^- and NO, and/or increasing those involved in the reduction of N_2O to N_2. These changes in microbial populations could be due to the direct effect of NIs on denitrifying microorganisms or due to the indirect effect of reducing the availability of NO_3^-. Therefore, the addition of DMPSA could be effective when conditions are favourable for high N_2O losses, e.g., significant SOM mineralization rates stimulated from the addition of N fertilizers (Thilakarathna and Hernandez-Ramirez, 2021) and even when a NO_3^--N-based synthetic fertilizer is applied. With regards to the effect of tillage, non-tilled microplots tended to reduce N_2O losses from ^{15}AN (compared with conventional tillage) but only when DMPSA was applied (Table 3, $P < 0.10$). Therefore, our findings were consistent with those of Corrochano-Monsalve et al. (2020) under a humid Mediterranean climate, suggesting that the combination of both strategies could be a good option for mitigating N_2O emissions.

4.2.2. *Emissions after harvest*

Under our climate and soil conditions, the highest N_2O flux regardless of fertilization or soil management was observed two months after harvest (Fig. 4b), after an intense rainfall event that was preceded by several weeks of drought and elevated temperatures (Fig. 1a). This pulse effect has been reported in several field studies under similar climatic conditions (Montoya et al., 2021; Montoya et al., 2022). The intensity of N_2O peaks after rewetting is greater when the soil remains close to the permanent wilting point during several weeks both with (Bergstermann et al., 2011) and without fertilizer application (Barrat et al., 2021), as was the case in our experiment.

The accumulated N_2O emissions derived from that pulse effect represented 71.5% of the total N_2O emissions, on average, thus highlighting the importance of measuring N_2O fluxes during the postharvest period in semiarid regions. Neither the fertilizer source (except the low peak in NT-N0) nor the tillage management affected the magnitude of the rewetting peak. Moreover, most of the N_2O released after harvest came from endogenous N rather than from the applied fertilizer (Table 3). This result could suggest that i) the opportunities for abating these rewetting peaks through fertilization or tillage management could be limited; ii) this type of peak could be mostly explained by the reactivation of microorganisms after rewetting (Priemé and Christensen, 2001; Barrat et al., 2021; Montoya et al., 2022) rather than by the accumulation of residual or surplus N. However, we speculate that denitrifying microorganisms could have played a significant role in the evolution of this peak because i) N_2O emissions derived from the NO_3^--N applied at top-dressing fertilization were higher than those derived from NH_4^+-N (in contrast with the trend observed before harvest) and ii) the mean NH_4^+ concentration at the rewetting event (0.8 mg N kg^{-1}) was much lower than that of NO_3^- (24.0 mg N kg^{-1}). The recent study of Montoya et al. (2022) also reported an increase in the abundance of nitrifying archaea and denitrifying populations (but not of nitrifying bacteria) during a postharvest rewetting peak.

4.3. *Plant N recovery*

Most N uptake of barley plants was obtained from soil/endogenous N instead of the N applied through top-dressing fertilization (Table 4). This result is in accordance with the review of Gardner and Drinkwater (2009). It is important to highlight that ^{15}N application was performed at top-dressing, but the crop also received a basal fertilization of 40 kg N ha^{-1} at seeding. This fact could partially explain our lower values compared with the 42% of plant N recovery and the 37% of N uptake derived from fertilizer reported for small grain crops by Yan et al. (2020). In addition, the fertilizer N losses that were not accounted for, e.g., NH_3 volatilization, N leaching, denitrification, could have also contributed to explaining the low N recoveries in barley (Harmsen, 2003). Both the % ^{15}N and the N derived from fertilizer in the crop (Table 4) revealed that barley plants preferably took up N from NO_3^- fertilization rather than from NH_4^+. These results are in accordance with those from Inselsbacher et al. (2013) in a barley crop and with those from Liu et al. (2019) in wheat cultivated in an alkaline soil.

Our results were also in accordance with most studies reviewed by Smith and Chalk (2020), in which tillage management did not affect fertilizer N recovery by crops, and with the *meta*-analysis of Gardner and Drinkwater (2009), which concluded that the use of NIs had no significant impact on crop N recovery. The *meta*-analysis by Sha et al. (2020) suggested that the use of NIs can enhance the crop recovery of N from fertilizer, particularly when applied with organic fertilizers or urea in soils with medium soil organic matter contents and neutral pH, rather than in soils with low organic matter content and calcareous soils, as in our experiment. Moreover, this *meta*-analysis reported that DMPP, did not have a significant effect on fertilizer-N recovery.

The use of DMPSA combined with no tillage enhanced the plant uptake of endogenous N, particularly in the grain (Table 4). This increase was attributable to the improvement of plant development and yields, rather than an effect on plant N concentrations. The results of the study by Montoya et al. (2022) under similar experimental conditions (see section 2.1 and Fig. S1) reported an increase of ca. 60% in barley biomass and grain yields in NT compared with T plots regardless of the

application of NIs in the fertilized treatments. The increase in N uptake and crop yield in non-tilled compared with tilled plots was also reported in the review of Shakoor et al. (2021) or by e.g., Soon and Arshad (2005) or Pittelkow et al. (2015) during dry years (as in our study) and/or in rainfed crops. This has also been observed under Mediterranean conditions (Morell et al., 2011; Plaza-Bonilla et al., 2014), being attributed to the improvement of chemical fertility and water retention capacity (Abdalla et al., 2016). The *meta*-analyses by Li et al. (2018) suggest that the enhancement in crop yield and/or NUE when applying NIs tend to diminish with high soil pH (>8) such as that of our study, and also that NIs are apparently more effective in enhancing NUE in irrigated cropping systems compared with rainfed ones. Recent studies using DMPSA did not find effects on crop yield in neither irrigated (Allende-Montalbán et al., 2022) nor rainfed (Guardia et al., 2020) cropping systems under Mediterranean climatic conditions.

4.4. Soil N at the end of the experimental period

Soil N that was derived from ^{15}AN fertilization was preferably retained in the topsoil (0–10 cm) (Fig. 6), which could be related to the adsorption capacity of NH_4^+ to the soil colloid, thus partially preventing its lixiviation to deeper layers. The concentration of soil N derived from fertilizer NH_4^+-N was higher than that derived from NO_3^--N fertilization in the first 10 cm, but the opposite trend was observed at 10–40 cm, thus indicating the higher leaching potential and mobility of synthetic NO_3^--N-based fertilizers (Fig. 6). This higher concentration of residual N derived from fertilizer NH_4^+-N fertilization in the top layer could also be related to the abovementioned barley preference of NO_3^- uptake by roots. It should be highlighted that under the conditions of the study, a significant amount of residual mineral N was present at the end of the experiment (Table S2).

The use of DMPSA significantly increased the topsoil retention of N-derived NH_4^+-N fertilization (Fig. 6), thus enhancing the potential biological uptake and adsorption by the soil matrix (Sha et al., 2020). Regarding tillage management, the higher residual N contents in the deepest layer in tilled plots could be related to the lower N uptake in comparison with no tillage and the vertical movement of this non-absorbed N. These results support the recommendation of combining no tillage and nitrification inhibitors such as DMPSA to reduce the environmental impacts during current and subsequent cropping campaigns.

Rainfed Mediterranean croplands are characterized by high inter-annual variability in the amount and distribution of precipitation. The present study took place during a dry campaign. However, different dynamics could be expected in humid campaigns. For instance, rainy seasons may stimulate aboveground and belowground biomass production, thus increasing plant N recovery. On the other hand, leaching losses are expected to increase under high-rainfall conditions, thus possibly decreasing both soil and plant recovery in coarse well-drained soils (Quemada et al., 2013). Moreover, the input of endogenous N from the mineralization of organic matter and crop residues is evidently driven by soil water availability (Quemada and Gabriel, 2016). To explore and disentangle these dynamics, further research is required under contrasting meteorological and soil (i.e., texture, pH) conditions.

5. Conclusions

During a dry campaign under rainfed semiarid conditions, N_2O emissions were mainly driven by a postharvest rewetting peak, while the study of the fate of fertilizer-^{15}N revealed low N recovery in plants and significant N recovery in the soil pool at the end of the experimental period. Therefore, the opportunities for climate change mitigation and adaptation from conservation agriculture practices or the use of nitrification inhibitors under these conditions could be very limited. However, the combination of DMPSA with no tillage could improve crop development and plant N uptake (no tillage) and increase N retention of the non-absorbed N fertilizer in the upper soil layers (DMPSA), thus reducing potential environmental impacts (e.g., N leaching) in subsequent seasons. The significant mitigation of N_2O (from both endogenous and exogenous N) during the growing season suggests that DMPSA is also a good N_2O mitigation strategy, if the emission pattern is different from that observed in our study (i.e., if most of the N_2O emissions occur after N fertilization and before harvest) and when a significant amount of N_2O is derived from soil, previous crop residues or residual N. Therefore, combining DMPSA with no tillage (when and where this tillage system improves crop development and N acquisition) could be considered a good strategy under a wide range of environmental conditions.

Declaration of Competing Interest

The authors declare that they have no known competing financial interests or personal relationships that could have appeared to influence the work reported in this paper.

Data availability

Data will be made available on request.

Acknowledgements

This research was funded by the project RTI2018-096267-B-I00 funded by Ministerio de Ciencia, Innovación y Competitividad (MCIN)/Agencia Estatal de Investigación (AEI)/10.13039/501100011033/Fondo Europeo de Desarrollo Regional (FEDER) "Una manera de hacer Europa", the Comunidad de Madrid (Spain) and Structural Funds 2014–2020 (ERDF and ESF) (project AGRISOST-CM S2018/BAA-4330). Funding for this research was also provided by EuroChemAgro GmbH. The Rothamsted Research contribution was supported by the BBSRC (grants BBS/E/C/000I0310 and BBS/E/C/000I0320). S. García-Gutiérrez is recipient of the FPI grant PRE2019-087594 funded by MCIN/AEI/10.13039/501100011033 and Fondo Social Europeo (FSE) "El FSE invierte en tu futuro". M. Montoya is recipient of the Margarita Salas grant of the Ministerio de Universidades and Universidad Politécnica de Madrid (RD 289/2021) supported by European Union-NextGenerationEU. Special thanks are given to the field assistants at Centro Nacional de Tecnología de Regadíos (CENTER), particularly to Alejandro Sánchez de Ribera, to the technicians at the Department of Chemistry and Food Technology of the ETSIAAB, Rocío Rodríguez, Estrella Revenga, Ana María Ros and Paloma Martín, and to Liz Dixon at the Rothamsted Research for the $^{15}N_2O$ analyses. Funding for open access charge: Universidad Politécnica de Madrid/Consorcio Madroño. This work was carried out within the framework of the Moncloa Campus of International Excellence (UCM-UPM).

Appendix A. Supplementary data

Supplementary data to this article can be found online at https://doi.org/10.1016/j.geoderma.2023.116424.

References

Abalos, D., Sanz-Cobena, A., Garcia-Torres, L., van Groenigen, J.W., Vallejo, A., 2013. Role of maize stover incorporation on nitrogen oxide emissions in a non-irrigated Mediterranean barley field. Plant and Soil 364, 357–371. https://doi.org/10.1007/s11104-012-1367-4.

Abdalla, K., Chivenge, P., Ciais, P., Chaplot, V., 2016. No-tillage lessens soil CO2 emissions the most under arid and sandy soil conditions: results from a meta-analysis. Biogeosciences 13, 3619–3633. https://doi.org/10.5194/bg-13-3619-2016.

Aguilera, E., Lassaletta, L., Sanz-Cobena, A., Garnier, J., Vallejo, A., 2013. The potential of organic fertilizers and water management to reduce N2O emissions in Mediterranean climate cropping systems. A review. Agriculture, Ecosystems and Environment 164, 32–52. https://doi.org/10.1016/j.agee.2012.09.006.

Allende-Montalbán, R., Martín-Lammerding, D., del Mar Delgado, M., Porcel, M.A., Gabriel, J.L., 2022. Nitrate Leaching in Maize (Zea mays L.) and Wheat (Triticum aestivum L.) Irrigated Cropping Systems under Nitrification Inhibitor and/or Intercropping Effects. Agriculture 12, 478. https://doi.org/10.3390/agriculture12040478.

Barrat, H.A., Evans, J., Chadwick, D.R., Clark, I.M., Le Cocq, K., Cardenas, M., L.,, 2021. The impact of drought and rewetting on N2O emissions from soil in temperate and Mediterranean climates. European Journal of Soil Science 72, 2504–2516. https://doi.org/10.1111/ejss.13015.

Barrena, I., Menéndez, S., Correa-Galeote, D., Vega-Mas, I., Bedmar, E.J., González-Murua, C., Estavillo, J.M., 2017. Soil water content modulates the effect of the nitrification inhibitor 3,4-dimethylpyrazole phosphate (DMPP) on nitrifying and denitrifying bacteria. Geoderma 303, 1–8. https://doi.org/10.1016/j.geoderma.2017.04.022.

Bergstermann, A., Cárdenas, L., Bol, R., Gilliam, L., Goulding, K., Meijide, A., Scholefield, D., Vallejo, A., Well, R., 2011. Effect of antecedent soil moisture conditions on emissions and isotopologue distribution of N2O during denitrification. Soil Biology and Biochemistry 43, 240–250. https://doi.org/10.1016/j.soilbio.2010.10.003.

Berhane, M., Xu, M., Liang, Z., Shi, J., Wei, G., Tian, X., 2020. Effects of long-term straw return on soil organic carbon storage and sequestration rate in North China upland crops: A meta-analysis. Global Change Biology 26, 2686–2701. https://doi.org/10.1111/gcb.15018.

Butterbach-Bahl, K., Baggs, E.M., Dannenmann, M., Kiese, R., Zechmeister-Boltenstern, S., 2013. Nitrous oxide emissions from soils: How well do we understand the processes and their controls? Philosophical Transactions of the Royal Society B: Biological Sciences 368. https://doi.org/10.1098/rstb.2013.0122.

Cayuela, M.L., Aguilera, E., Sanz-Cobena, A., Adams, D.C., Ábalos, D., Barton, L., Ryals, R., Silver, W.L., Alfaro, M.A., Pappa, V.A., Smith, P., Garnier, J., Billen, G., Bouwman, L., Bondeau, A., Lassaletta, L., 2017. Direct nitrous oxide emissions in Mediterranean climate cropping systems: Emission factors based on a meta-analysis of available measurement data. Agriculture, Ecosystems and Environment 238, 25–35. https://doi.org/10.1016/j.agee.2016.10.006.

Cheng, Y., Elrys, A.S., Wang, J., Xu, C., Ni, K., Zhang, J., Wang, S., Cai, Z., Pacholski, A., 2022. Application of enhanced-efficiency nitrogen fertilizers reduces mineral nitrogen usage and emissions of both N2O and NH3 while sustaining yields in a wheat-rice rotation system. Agriculture, Ecosystems & Environment 324, 107720. https://doi.org/10.1016/j.agee.2021.107720.

Corrochano-Monsalve, M., Huérfano, X., Menéndez, S., Torralbo, F., Fuertes-Mendizábal, T., Estavillo, J.M., González-Murua, C., 2020. Relationship between tillage management and DMPSA nitrification inhibitor efficiency. Science of the Total Environment 718. https://doi.org/10.1016/j.scitotenv.2019.134748.

Couto-Vázquez, A., González-Prieto, S.J., 2016. Fate of 15 N-fertilizers in the soil-plant system of a forage rotation under conservation and plough tillage. Soil and Tillage Research 161, 10–18. https://doi.org/10.1016/j.still.2016.02.011.

Cowan, N., Levy, P., Drewer, J., Carswell, A., Shaw, R., Simmons, I., Bache, C., Marinheiro, J., Brichet, J., Sanchez-Rodriguez, A.R., Cotton, J., Hill, P.W., Chadwick, D.R., Jones, D.L., Misselbrook, T.H., Skiba, U., 2019. Application of Bayesian statistics to estimate nitrous oxide emission factors of three nitrogen fertilisers on UK grasslands. Environment International 128, 362–370. https://doi.org/10.1016/j.envint.2019.04.054.

Elrys, A.S., Ali, A., Zhang, H., Cheng, Y., Zhang, J., Cai, Z.C., Müller, C., Chang, S.X., 2021. Patterns and drivers of global gross nitrogen mineralization in soils. Global Change Biology 27, 5950–5962. https://doi.org/10.1111/gcb.15851.

Foster, P., Storelvmo, T., Armour, K., Collins, W., Dufresne, J.-L., Frame, D., Lunt, D.J., Mauritsen, T., Palmer, M.D., Watanabe, M., Wild, M., Zhang, H., 2021. The Earth's Energy Budget, Climate Feedbacks, and Climate Sensitivity, in: Climate Change 2021: The Physical Science Basis. Contribution of Working Group I to the Sixth Assessment Report of the Intergovernmental Panel on Climate Change. [Masson-Delmotte, V., P. Zhai, A. Pirani, S.L. Connors, C. Péan, S. Berger, N. Caud, Y. Chen, L. Goldfarb, M.I. Gomis, M. Huang, K. Leitzell, E. Lonnoy, J.B.R. Matthews, T.K. Maycock, T. Waterfield, O. Yelekçi, R. Yu, and B. Zhou (Eds.)]. Cambridge University Press, Cambridge, United Kingdom and New York, NY, USA, pp. 923-1054. doi: 10.1017/9781009157896.009.

García-Gómez, C., Babín, M., Obrador, A., Álvarez, J.M., Fernández, M.D., 2015. Integrating ecotoxicity and chemical approaches to compare the effects of ZnO nanoparticles, ZnO bulk, and ZnCl2 on plants and microorganisms in a natural soil. Environmental Science and Pollution Research 22, 16803–16813. https://doi.org/10.1007/s11356-015-4867-y.

Gardner, J.B., Drinkwater, L.E., 2009. The fate of nitrogen in grain cropping systems: A meta-analysis of 15N field experiments. Ecological Applications 19, 2167–2184. https://doi.org/10.1890/08-1122.1.

Geens, E.L., Davies, G.P., Maggs, J.M., Barraclough, D., 1991. The use of mean pool abundances to interpret 15N tracer experiments. Plant and Soil 131, 97–105. https://doi.org/10.1007/BF00010424.

Guardia, G., Vallejo, A., Cárdenas, L.M., Dixon, E.R., García-Marco, S., 2018. Fate of 15N-labelled ammonium nitrate with or without the new nitrification inhibitor DMPSA in an irrigated maize crop. Soil Biology and Biochemistry 116, 193–202. https://doi.org/10.1016/j.soilbio.2017.10.013.

Guardia, G., González-Murua, C., Fuertes-Mendizábal, T., Vallejo, A., 2020. The scarcity and distribution of rainfall drove the performance (i.e., mitigation of N oxide emissions, crop yield and quality) of calcium ammonium nitrate management in a wheat crop under rainfed semiarid conditions. Archives of Agronomy and Soil Science 66, 1827–1844. https://doi.org/10.1080/03650340.2019.1697805.

Guardia, G., García-Gutiérrez, S., Rodríguez-Pérez, R., Recio, J., Vallejo, A., 2021. Increasing N use efficiency while decreasing gaseous N losses in a non-tilled wheat (Triticum aestivum L.) crop using a double inhibitor. Agriculture, Ecosystems and Environment 319. https://doi.org/10.1016/j.agee.2021.107546.

Guzman-Bustamante, I., Schulz, R., Müller, T., Ruser, R., 2022. Split N application and DMP based nitrification inhibitors mitigate N2O losses in a soil cropped with winter wheat. Nutrient Cycling in Agroecosystems 123, 119–135. https://doi.org/10.1007/s10705-022-10211-7.

Harmsen, K., 2003. A comparison of the isotope-dilution and the difference method for estimating fertilizer nitrogen recovery fractions in crops. I. Plant uptake and loss of nitrogen. Netherlands Journal of Agricultural Science 50, 321–347. https://doi.org/10.1016/s1573-5214(03)80015-5.

Hart, S.C., Stark, J.M., Davidson, E.A., Firestone, M.K., 1994. Nitrogen mineralization, immobilization, and nitrification, in: Weaver, R.W., Angle, S., Bottomley, P., Bezdicek, D., Smith, S., Tabatabai, A., Wollum, A. (Eds.), Methods of Soil Analysis: Part 2 Microbiological and Biochemical Properties. pp. 985–1018. doi:10.2136/sssabookser5.2.c42.

Harty, M.A., McGeough, K.L., Carolan, R., Müller, C., Laughlin, R.J., Lanigan, G.J., Richards, K.G., Watson, C.J., 2017. Gross nitrogen transformations in grassland soil react differently to urea stabilisers under laboratory and field conditions. Soil Biology and Biochemistry 109, 23–34. https://doi.org/10.1016/j.soilbio.2017.01.025.

He, X., Chi, Q., Cai, Z., Cheng, Y., Zhang, J., Müller, C., 2020. 15N tracing studies including plant N uptake processes provide new insights on gross N transformations in soil-plant systems. Soil Biology and Biochemistry 141, 107666. https://doi.org/10.1016/j.soilbio.2019.107666.

Huang, Y., Ren, W., Wang, L., Hui, D., Grove, J.H., Yang, X., Tao, B., Goff, B., 2018. Greenhouse gas emissions and crop yield in no-tillage systems: A meta-analysis. Agriculture, Ecosystems & Environment 268, 144–153. https://doi.org/10.1016/j.agee.2018.09.002.

Huérfano, X., Fuertes-Mendizábal, T., Fernández-Diez, K., Estavillo, J.M., González-Murua, C., Menéndez, S., 2016. The new nitrification inhibitor 3, 4-dimethylpyrazole succinic (DMPSA) as an alternative to DMPP for reducing N2O emissions from wheat crops under humid Mediterranean conditions. European Journal of Agronomy 80, 78–87. https://doi.org/10.1016/j.eja.2016.07.001.

Huérfano, X., Estavillo, J.M., Torralbo, F., Vega-Mas, I., González-Murua, C., Fuertes-Mendizábal, T., 2022. Dimethylpyrazole-based nitrification inhibitors have a dual role in N2O emissions mitigation in forage systems under Atlantic climate conditions. Science of The Total Environment 807, 150670. https://doi.org/10.1016/j.scitotenv.2021.150670.

Inselsbacher, E., Wanek, W., Strauss, J., Zechmeister-Boltenstern, S., Müller, C., 2013. A novel 15N tracer model reveals: Plant nitrate uptake governs nitrogen transformation rates in agricultural soils. Soil Biology and Biochemistry 57, 301–310. https://doi.org/10.1016/j.soilbio.2012.10.010.

IPCC, 2022. Climate Change 2022: Mitigation of Climate Change. Working Group III Contribution to the IPCC Sixth Assessment Report. [P.R. Shukla, J. Skea, R. Slade, A. Al Khourdajie, R. van Diemen, D. McCollum, M. Pathak, S. Some, P. Vyas, R. Fradera, M. Belkacemi, A. Hasija, G. Lisboa, S. Luz, J. Malley, (eds.)]. Cambridge University Press, Cambridge, UK and New York, NY, USA. doi:10.1017/9781009157926.

Kirkham, D., Bartholomew, W.V., 1954. Equations for Following Nutrient Transformations in Soil. Utilizing Tracer Data. Soil Science Society of America Journal 18, 33–34. https://doi.org/10.2136/sssaj1954.03615995001800010009x.

Li, T., Zhang, W., Yin, J., Chadwick, D., Norse, D., Lu, Y., Liu, X., Chen, X., Zhang, F., Powlson, D., Dou, Z., 2018. Enhanced-efficiency fertilizers are not a panacea for resolving the nitrogen problem. Global Change Biology. 24. e511–e521. doi: 10.1111/gcb.13918.

Li, Y., Ju, X., Wu, D., 2023. Transient nitrite accumulation explains the variation of N2O emissions to N fertilization in upland agricultural soils. Soil Biology and Biochemistry 177, 108917. https://doi.org/10.1016/j.soilbio.2022.108917.

Li, X., Sørensen, P., Olesen, J.E., Petersen, S.O., 2016. Evidence for denitrification as main source of N2O emission from residue-amended soil. Soil Biology and Biochemistry 92, 153–160. https://doi.org/10.1016/j.soilbio.2015.10.008.

Liu, S., Chi, Q., Cheng, Y., Zhu, B., Li, W., Zhang, X., Huang, Y., Müller, C., Cai, Z., Zhang, J., 2019. Importance of matching soil N transformations, crop N form preference, and climate to enhance crop yield and reducing N loss. Science of the Total Environment 657, 1265–1273. https://doi.org/10.1016/j.scitotenv.2018.12.100.

Marsden, K.A., Marín-Martínez, A.J., Vallejo, A., Hill, P.W., Jones, D.L., Chadwick, D.R., 2016. The mobility of nitrification inhibitors under simulated ruminant urine deposition and rainfall: a comparison between DCD and DMPP. Biology and Fertility of Soils 52, 491–503. https://doi.org/10.1007/s00374-016-1092-x.

Montoya, M., Vallejo, A., Corrochano-Monsalve, M., Aguilera, E., Sanz-Cobena, A., Ginés, C., González-Murua, C., Álvarez, J.M., Guardia, G., 2021. Mitigation of yield-scaled nitrous oxide emissions and global warming potential in an oilseed rape crop through N source management. Journal of Environmental Management 288. https://doi.org/10.1016/j.jenvman.2021.112304.

Montoya, M., Juhanson, J., Hallin, S., García-Gutiérrez, S., García-Marco, S., Vallejo, A., Recio, J., Guardia, G., 2022. Nitrous oxide emissions and microbial communities during the transition to conservation agriculture using N-enhanced efficiency fertilisers in a semiarid climate. Soil Biology and Biochemistry 170, 108687. https://doi.org/10.1016/j.soilbio.2022.108687.

Morell, F.J., Lampurlanés, J., Álvaro-Fuentes, J., Cantero-Martínez, C., 2011. Yield and water use efficiency of barley in a semiarid Mediterranean agroecosystem: Long-term effects of tillage and N fertilization. Soil and Tillage Research 117, 76–84. https://doi.org/10.1016/j.still.2011.09.002.

Murphy, D.V., Recous, S., Stockdale, E.A., Fillery, I.R.P., Jensen, L.S., Hatch, D.J., Goulding, K.W.T., 2003. Gross nitrogen fluxes in soil: theory, measurement and

application of 15N pool dilution techniques. Advances in Agronomy 79, 69–118. https://doi.org/10.1016/S0065-2113(02)79002-0.
Pacholski, A., Berger, N., Bustamante, I., Ruser, R., Guardia, G., Mannheim, T., 2016. Effects of the novel nitrification inhibitor DMPSA on yield, mineral N dynamics and N2O emissions, in: Proceedings of the 2016 International Nitrogen Initiative Conference, "Solutions to Improve Nitrogen Use Efficiency for the World", 4 – 8 December 2016, Melbourne, Australia.
Pan, B., Lam, S.K., Mosier, A., Luo, Y., Chen, D., 2016. Ammonia volatilization from synthetic fertilizers and its mitigation strategies: A global synthesis. Agriculture, Ecosystems & Environment 232, 283–289. https://doi.org/10.1016/j.agee.2016.08.019.
Paniagua, L.L., García-Martín, A., Moral, F.J., Rebollo, F.J., 2019. Aridity in the Iberian Peninsula (1960–2017): distribution, tendencies, and changes. Theoretical and Applied Climatology 138, 811–830. https://doi.org/10.1007/s00704-019-02866-0.
Petersen, S.O., Nielsen, T.H., Frostegård, Å., Olesen, T., 1996. O2 uptake, C metabolism and denitrification associated with manure hot-spots. Soil Biology and Biochemistry 28, 341–349. https://doi.org/10.1016/0038-0717(95)00150-6.
Pilegaard, K., 2013. Processes regulating nitric oxide emissions from soils. Philosophical Transactions of the Royal Society B: Biological Sciences 368, 20130126. https://doi.org/10.1098/rstb.2013.0126.
Pinheiro, P.L., Recous, S., Dietrich, G., Weiler, D.A., Giovelli, R.L., Mezzalira, A.P., Giacomini, S.J., 2018. Straw removal reduces the mulch physical barrier and ammonia volatilization after urea application in sugarcane. Atmospheric Environment 194, 179–187. https://doi.org/10.1016/j.atmosenv.2018.09.031.
Pittelkow, C.M., Liang, X., Linquist, B.A., van Groenigen, K.J., Lee, J., Lundy, M.E., van Gestel, N., Six, J., Venterea, R.T., van Kessel, C., 2015. Productivity limits and potentials of the principles of conservation agriculture. Nature 517, 365–368. https://doi.org/10.1038/nature13809.
Plaza-Bonilla, D., Álvaro-Fuentes, J., Arrúe, J.L., Cantero-Martínez, C., 2014. Tillage and nitrogen fertilization effects on nitrous oxide yield-scaled emissions in a rainfed Mediterranean area. Agriculture, Ecosystems and Environment 189, 43–52. https://doi.org/10.1016/j.agee.2014.03.023.
Priemé, A., Christensen, S., 2001. Natural perturbations, drying-wetting and freezing-thawing cycles, and the emission of nitrous oxide, carbon dioxide and methane from farmed organic soils. Soil Biology and Biochemistry 33, 2083–2091. https://doi.org/10.1016/S0038-0717(01)00140-7.
Qiao, C., Liu, L., Hu, S., Compton, J.E., Greaver, T.L., Li, Q., 2015. How inhibiting nitrification affects nitrogen cycle and reduces environmental impacts of anthropogenic nitrogen input. Global Change Biology 21, 1249–1257. https://doi.org/10.1111/gcb.12802.
Quemada, M., Baranski, M., Nobel-de Lange, M.N.J., Vallejo, A., Cooper, J.M., 2013. Meta-analysis of strategies to control nitrate leaching in irrigated agricultural systems and their effects on crop yield. Agriculture, Ecosystems & Environment 174, 1–10. https://doi.org/10.1016/j.agee.2013.04.018.
Quemada, M., Gabriel, J.L., 2016. Approaches for increasing nitrogen and water use efficiency simultaneously. Global Food Security 9, 29–35. https://doi.org/10.1016/j.gfs.2016.05.004.
Quemada, M., Lassaletta, L., Jensen, L.S., Godinot, O., Brentrup, F., Buckley, C., Foray, S., Hvid, S.K., Oenema, J., Richards, K.G., Oenema, O., 2020. Exploring nitrogen indicators of farm performance among farm types across several European case studies. Agricultural Systems 177. https://doi.org/10.1016/j.agsy.2019.102689.
Ravishankara, A., Daniel, J., Portman, R., 2009. Nitrous Oxide (N2O): The Dominant Ozone-Depleting Substance Emitted in the 21st Century. Science 326, 123–125. https://doi.org/10.1126/science.1176985.
Roman-Perez, C.C., Hernandez-Ramirez, G., 2021. Sources and priming of nitrous oxide production across a range of moisture contents in a soil with high organic matter. Journal of Environmental Quality 50, 94–109. https://doi.org/10.1002/jeq2.20172.
Ruppel, S., Jürgen, A., Graefe, J., Rühlmann, J., Peschke, H., 2006. Gross N transfer rates in field soils measured by dilution N-pool. Archives of Agronomy and Soil Science 52, 377–388. https://doi.org/10.1080/03650340600849357.
Ruser, R., Schulz, R., 2015. The effect of nitrification inhibitors on the nitrous oxide (N2O) release from agricultural soils-a review. Journal of Plant Nutrition and Soil Science 178, 171–188. https://doi.org/10.1002/jpln.201400251.
Schleusner, P., Lammirato, C., Tierling, J., Lebender, U., Rütting, T., 2018. Primed N_2O emission from native soil nitrogen: A ^{15}N-tracing laboratory experiment. Journal of Plant Nutrition and Soil Science 181, 621–627. https://doi.org/10.1002/jpln.201700312.
Sha, Z., Ma, X., Wang, J., Lv, T., Li, Q., Misselbrook, T., Liu, X., 2020. Effect of N stabilizers on fertilizer-N fate in the soil-crop system: A meta-analysis. Agriculture, Ecosystems and Environment 290. https://doi.org/10.1016/j.agee.2019.106763.
Shakoor, A., Shahbaz, M., Farooq, T.H., Sahar, N.E., Shahzad, S.M., Altaf, M.M., Ashraf, M., 2021. A global meta-analysis of greenhouse gases emission and crop yield under no-tillage as compared to conventional tillage. Science of The Total Environment 750, 142299. https://doi.org/10.1016/j.scitotenv.2020.142299.
Smith, C.J., Chalk, P.M., 2020. The role of 15N in tracing N dynamics in agro-ecosystems under alternative systems of tillage management: A review. Soil and Tillage Research 197, 104496. https://doi.org/10.1016/j.still.2019.104496.
Smith, P., Martino, D., Cai, Z., Gwary, D., Janzen, H., Kumar, P., McCarl, B., Ogle, S., O'Mara, F., Rice, C., Scholes, B., Sirotenko, O., Howden, M., McAllister, T., Pan, G., Romanenkov, V., Schneider, U., Towprayoon, S., Wattenbach, M., Smith, J., 2008. Greenhouse gas mitigation in agriculture. Philosophical Transactions of the Royal Society B: Biological Sciences 363, 789–813. https://doi.org/10.1098/rstb.2007.2184.
Soil Survey Staff, 2014. Keys to Soil Taxonomy, 12th ed. Change. 327–328.
Soon, Y.K., Arshad, M.A., 2005. Tillage and liming effects on crop and labile soil nitrogen in an acid soil. Soil and Tillage Research 80, 23–33. https://doi.org/10.1016/j.still.2004.02.017.
Souza, E.F.C., Rosen, C.J., Venterea, R.T., 2021. Co-application of DMPSA and NBPT with urea mitigates both nitrous oxide emissions and nitrate leaching during irrigated potato production. Environmental Pollution 284, 117124. https://doi.org/10.1016/j.envpol.2021.117124.
Thilakarathna, S.K., Hernandez-Ramirez, G., 2021. How does management legacy, nitrogen addition, and nitrification inhibition affect soil organic matter priming and nitrous oxide production? Journal of Environmental Quality 50, 78–93. https://doi.org/10.1002/jeq2.20168.
Thompson, R.L., Lassaletta, L., Patra, P.K., Wilson, C., Wells, K.C., Gressent, A., Koffi, E.N., Chipperfield, M.P., Winiwarter, W., Davidson, E.A., Tian, H., Canadell, J.G., 2019. Acceleration of global N2O emissions seen from two decades of atmospheric inversion. Nature Climate Change 9, 993–998. https://doi.org/10.1038/s41558-019-0613-7.
Torralbo, F., Menéndez, S., Barrena, I., Estavillo, J.M., Marino, D., González-Murua, C., 2017. Dimethyl pyrazol-based nitrification inhibitors effect on nitrifying and denitrifying bacteria to mitigate N2O emission. Scientific Reports 7, 13810. https://doi.org/10.1038/s41598-017-14225-y.
Unkovich, M., Jamieson, N., Monaghan, R., Barraclough, D., 1998. Nitrogen mineralisation and plant nitrogen acquisition in a nitrogen-limited calcereous grassland. Environmental and Experimental Botany 40, 209–219. https://doi.org/10.1016/S0098-8472(98)00038-0.
Ussiri, D., Lal, R., 2013. Soil Emission of Nitrous Oxide and its Mitigation. Springer Science & Business Media.
Volpi, I., Laville, P., Bonari, E., di Nasso, N.N., o, Bosco, S.,, 2017. Improving the management of mineral fertilizers for nitrous oxide mitigation: The effect of nitrogen fertilizer type, urease and nitrification inhibitors in two different textured soils. Geoderma 307, 181–188. https://doi.org/10.1016/j.geoderma.2017.08.018.
Wang, S., Luo, S., Yue, S., Li, S., 2016. Fate of 15N fertilizer under different nitrogen split applications to plastic mulched maize in semiarid farmland. Nutrient Cycling in Agroecosystems 105, 129–140. https://doi.org/10.1007/s10705-016-9780-3.
Xia, L., Lam, S.K., Chen, D., Wang, J., Tang, Q., Yan, X., 2017. Can knowledge-based N management produce more staple grain with lower greenhouse gas emission and reactive nitrogen pollution? A meta-analysis. Global Change Biology 23, 1917–1925. https://doi.org/10.1111/gcb.13455.
Yan, M., Pan, G., Lavallee, J.M., Conant, R.T., 2020. Rethinking sources of nitrogen to cereal crops. Global Change Biology 26, 191–199. https://doi.org/10.1111/gcb.14908.
Yansheng, C., Fengliang, Z., Zhongyi, Z., Tongbin, Z., Huayun, X., 2020. Biotic and abiotic nitrogen immobilization in soil incorporated with crop residue. Soil and Tillage Research 202, 104664. https://doi.org/10.1016/j.still.2020.104664.
Zhu, G., Ju, X., Zhang, J., Müller, C., Rees, R.M., Thorman, R.E., Sylvester-Bradley, R., 2019. Effects of the nitrification inhibitor DMPP (3,4-dimethylpyrazole phosphate) on gross N transformation rates and N2O emissions. Biology and Fertility of Soils 55, 603–615. https://doi.org/10.1007/s00374-019-01375-6.